N78-24574

NASA Contractor Report 157137

STRESS INTENSITY FACTORS IN BONDED HALF PLANES CONTAINING INCLINED CRACKS AND SUBJECTED TO ANTIPLANE SHEAR LOADING

J. L. Bassani and F. Erdogan

LEHIGH UNIVERSITY
Bethlehem, PA 18015

NASA Grant NGR 39-007-011
April 1978

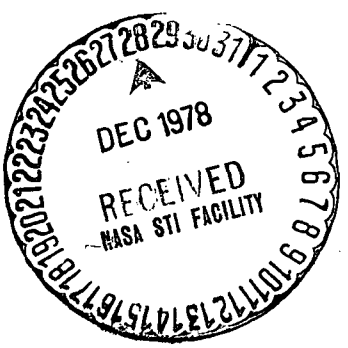

National Aeronautics and
Space Administration

Langley Research Center
Hampton, Virginia 23665

STRESS INTENSITY FACTORS IN BONDED HALF PLANES CONTAINING INCLINED CRACKS AND SUBJECTED TO ANTIPLANE SHEAR LOADING.*

by

J.L. Bassani and F. Erdogan
Lehigh University, Bethlehem, PA.

ABSTRACT

The antiplane shear problem for two bonded dissimilar half planes containing a semi-infinite crack or two arbitrarily located collinear cracks is considered. For the semi-infinite crack the problem is solved for a concentrated wedge load and the stress intensity factor and the angular distribution of stresses are calculated. For finite cracks the problem is reduced to a pair of integral equations. Numerical results are obtained for cracks fully imbedded in a homogeneous medium, one crack tip touching the interface, and a crack crossing the interface for various crack angles.

---

*This work was supported by NASA-Langley under the Grant NGR39-007-011 and by NSF under the Grant ENG-77-19127.

1. INTRODUCTION

In analytical studies relating to the fracture of structural solids, solutions of anit-plane shear problems serve two distinct purposes. First, they may be used to shed some light on the qualitative behavior of the solutions for the corresponding somewhat more difficult in-plane deformation problems. Secondly, they may have practical applications in their own right in situations such as torsion or three-dimensional problems in which the so-called third mode is separable. Particularly in the fracture of nonhomogeneous materials initiating from the flaws in the close neighborhood of phase boundaries, such as in the growth of microflaws in polycrystals and cracks in composites, the third mode of fracture may be quite important. With this in mind, it seemed to be worthwhile to report some new results regarding the anti-plane shear cracks in nonhomogeneous materials. The main problem is that of a slanted crack in the neighborhood of a plane bimaterial interface, including the geometries of the crack touching or crossing the interface. The cases of semi-infinite crack and the half plane consisting of two bonded wedges are also considered as they relate to the main problem.

The general antiplane shear problem is well-understood and the basic techniques dealing with its solution have been thoroughly documented in literature. Therefore, to include in this paper an exhaustive review of the subject and the details of the analysis did not seem to be necessary. The problem under consideration is the generalization of that considered in [1] where only the case

of the cracks perpendicular to the interface was studied. The general method has also been described in [2]. References on the crack and dislocation problems may be found in [1] and [2].

2. SEMI-INFINITE CRACK AND THE HALF PLANE

The anti-plane shear problems for bonded dissimilar half planes with a semi-infinite crack and for a half plane which consists of two dissimilar wedges are described in Figures 1 and 2. In the case of semi-infinite crack under a concentrated anti-plane shear loading given by

$$\tau_{1\theta z}(r,0) = \tau_{3\theta z}(r,0) = q\delta(r-r_0), \qquad (1)$$

using the standard Mellin transforms the solution may be found as

$$w_j(r,\theta) = \frac{1}{2\pi i}\int_{c-i\infty}^{c+i\infty}[A_j(s)\sin(s\theta)+B_j(s)\cos(s\theta)]r^{-s}ds,$$

$$\tau_{j\theta z}(r,\theta) = \frac{1}{2\pi i}\int_{c-i\infty}^{c+i\infty}\mu_j s[A_j(s)\cos(s\theta)-B_j(s)\sin(s\theta)]r^{-s-1}ds,$$

$$\tau_{jrz}(r,\theta) = \frac{-1}{2\pi i}\int_{c-i\infty}^{c+i\infty}\mu_j s[A_j(s)\sin(s\theta)+B_j(s)\cos(s\theta)]r^{-s-1}ds,$$

$$(j = 1,2,3) \quad . \quad (2a\text{-}c)$$

where w_j is the z-component of the displacement, $\tau_{j_{\theta z}}$ and $\tau_{j_{rz}}$ are the stresses in the jth wedge shown in Figure 1, and

$$A_1(s) = A_3(s) = \frac{qr_0^s}{s\mu_1},$$

$$A_2(s) = \frac{-\mu_1 A_1(s)\sin(2s\pi)}{\sin(s\pi)K(s)},$$

$$B_2(s) = \frac{\mu_1 A_1(s)[1-\cos(2s\pi)]}{\sin(s\pi)K(s)} \quad ,$$

$$B_3(s) = \frac{A_2(s)\sin[s(\theta_o+\pi)]+B_2(s)\cos[s(\theta_o+\pi)]-A_3(s)\sin[s(\theta_o-\pi)]}{\cos[s(\theta_o-\pi)]},$$

$$B_1(s) = \frac{A_2(s)\sin(s\theta_o)+B_2(s)\cos(s\theta_o)-A_1(s)\sin(s\theta_o)}{\cos(s\theta_o)} \quad , \qquad (3a\text{-}e)$$

$$K(s) = (\mu_1-\mu_2)\cos[s(\pi-2\theta_o)] - (\mu_1+\mu_2)\cos(s\pi) \quad , \qquad (4)$$

Of particular practical interest is the shear cleavage stress in the half plane 2 which, for $r<<r_o$, may be expressed in the following asymptotic form:

$$\tau_{2_{\theta z}}(r,\theta) = \frac{q}{r_o}\frac{G_{-1}(\theta)}{(r/r_o)^{\beta}} + O(r/r_o)^{s_2-1}) \quad , \beta=1-s_1 \quad , r<<r_o \quad ,$$

$$\theta_o<\theta<\theta_o+\pi \quad , \qquad (5)$$

$$G_{-1}(\theta) = \frac{-2\mu_2\cos[s_1(\pi-\theta)]}{(\mu_1-\mu_2)(\pi-2\theta_o)\sin[s_1(\pi-2\theta_o)]-(\mu_1+\mu_2)\pi\sin(s_1\pi)} \quad ,$$

$$(\theta_o\leq\theta\leq\theta_o+\pi) \quad . \qquad (6)$$

where s is the root of $K(s) = 0$ with $0<Re(s_1)<1$ and it can be shown that there is only one such root in this strip which is always real, and $Re(s_2)>1$. Table 1 shows the power of stress singularity for various material combinations and for various values of θ_o. Expressions similar to (5) can be developed for other stress components in the two materials. Figures 3-5 show some sample results for the function $G_{-1}(\theta)$ in the entire range $0<\theta<2\pi$. Analytically, it can be shown that $G_{-1}(\theta)$ becomes maximum for $\theta = \pi$ indicating that the plane of the crack is the weak shear cleavage plane in the bonded

medium. One may also note that (arbitrarily) defining a stress intensity factor by

$$k_3 = \lim_{r\to 0}\sqrt{2}\, r^{\beta}\, \tau_{2\theta z}(r,\pi) \quad , \tag{7}$$

it is seen that in this problem

$$k_3 = \sqrt{2}\, q\, r_o^{\beta-1}\, G_{-1}(\pi) \quad . \tag{8}$$

Also, referring to Figure 1 and defining the stress intensity factor in terms of the crack opening displacement as (see [1]),

$$k_3 = \lim_{r\to 0} \sqrt{2}\, \mu^* \frac{\partial}{\partial r} [w_1(r,+0) - w_3(r,-0)] \tag{9}$$

we find

$$\mu^* = \frac{-\mu_2 \cos(s_1\theta_o)\cos[s_1(\pi-\theta_o)]}{\sin[s_1(\pi-\theta_o)]\cos[s_1(\pi-\theta_o)]+\sin(s_1\theta_o)\cos(s_1\theta_o)} \quad . \tag{10}$$

Figure 6 shows an example for the angular distribution of the asymptotic values of τ_{rz} which, for the nonhomogeneous medium, is seen to be discontinuous at the interfaces $\theta = \theta_o$ and $\theta = \pi + \theta_o$.

For the half plane shown in Figure 2 the basic equations (2) are still valid where for the external load

$$\tau_{1\theta z}(r,-\theta_o) = q_1\delta(r-r_o), \tag{11}$$

the functions $A_i(s)$ and $B_i(s)$, $(i=1,2)$ are given by

$$A_1(s) = \frac{q_1 r_o^s \sin(s\theta_2)}{\mu_1 s K_1(s)} = \frac{\mu 2}{\mu_1} A_2(s) \quad ,$$

$$B_1(s) = \frac{q_1 r_o^s \cos(s\theta_2)}{\mu_2 s K_1(s)} = B_2(s) \quad , \ \theta_2 = \pi-\theta_o \quad , \tag{12}$$

$$K_1(s) = \frac{1}{2\mu_2}\{(\mu_1+\mu_2)\sin(s\pi) + (\mu_2-\mu_1)\sin[s(\pi-2\theta_o)]\} \quad . \tag{13}$$

Table 1. Power of stress singularity β, for a crack terminating at the interface. $\mu_2/\mu_1 = 0.0072$ for Boron-Epoxy, 0.043 for Aluminum-Epoxy, 1.0 for homogeneous medium, 23.08 for Epoxy-Aluminum, and 138.46 for Epoxy-Boron.

	μ_2/μ_1				
θ_o	0.0072	0.043	1.0	23.08	138.36
0	0.5	0.5	0.5	0.5	0.5
$\frac{\pi}{16}$	0.890	0.753	0.5	0.468	0.467
$\frac{\pi}{8}$	0.919	0.809	0.5	0.432	0.429
$\frac{3\pi}{16}$	0.931	0.836	0.5	0.391	0.386
$\frac{\pi}{4}$	0.938	0.851	0.5	0.344	0.335
$\frac{5\pi}{16}$	0.942	0.860	0.5	0.290	0.276
$\frac{3\pi}{8}$	0.944	0.865	0.5	0.228	0.205
$\frac{7\pi}{16}$	0.946	0.868	0.5	0.165	0.122
$\frac{\pi}{2}$	0.946	0.869	0.5	0.131	0.054

Table 2. Power of singularity β' at vertex for bonded wedges of total angle π.

θ_o	$\frac{\mu_1}{\mu_2} = 23.08$	$\frac{\mu_1}{\mu_2} = 138.46$
$\frac{\pi}{16}$	0.355	0.444
$\frac{2\pi}{16}$	0.367	0.417
$\frac{3\pi}{16}$	0.343	0.377
$\frac{4\pi}{16}$	0.303	0.328
$\frac{5\pi}{16}$	0.251	0.269
$\frac{6\pi}{16}$	0.185	0.197
$\frac{7\pi}{16}$	0.103	0.110

Examining the asymptotic behavior of the solution for $r<<r_o$, it can be shown that for $\theta_o<\pi/2$ the power β' of the dominant term is negative if $\mu_1<\mu_2$ (i.e., the stress state at $r = 0$ is bounded), and positive if $\mu_1>\mu_2$ (i.e., the stress state at $r = 0$ is singular). Near the apex the shear cleavage stress is (Figure 2)

$$\tau_{\theta z}(r,\theta) = \frac{q}{r_o}\ \frac{H_1(\theta)}{(r/r_o)^{\beta'}} + O(r/r_o)^{s_2-1}) \quad , \tag{14}$$

$$H_1(\theta) = \frac{(\mu_1-\mu_2)\sin[s_1(\theta_2-\theta)]-(\mu_1+\mu_2)\sin[s_1(\theta_2-\theta)]}{L(s_1)} \quad ,$$

$$H_2(\theta) = \frac{-2\mu_2\sin[s_1(\theta_2-\theta)]}{L(s_1)} \quad , \quad \theta_2 = \pi-\theta_o \quad , \tag{15}$$

$$L(s_1)=(\mu_1+\mu_2)\pi\cos(s_1\pi)+(\mu_2-\mu_1)(\pi-2\theta_o)\cos[s_1(\pi-2\theta_o)] \quad , \tag{16}$$

It can also be shown that the displacement derivatives and the cleavage shear along the bond line $\theta = 0$ are related by

$$\mu_1\ \frac{\partial}{\partial r}\ w_1(0,-\theta_o) = \{(\mu_1-\mu_2)\cos[s_1(\pi-2\theta_o)]$$

$$+ (\mu_1+\mu_2)\cos\ s_1\pi\}\ \frac{\partial}{\partial r}\ w_2(0,\pi-\theta_o) \quad . \tag{17}$$

$$\lim_{r\to 0} r^{\beta'}\tau_{1_{\theta z}}(r,0) = \lim_{r\to 0}\mu_1^*\ r^{\beta'}\ \frac{\partial}{\partial r}\ w_1(r,-\theta_o) \quad , \tag{18}$$

$$\mu_1^* = \frac{-2\mu_1\mu_2\sin[s_1(\pi-\theta_o)]}{(\mu_2-\mu_1)\cos[s_1(\pi-2\theta_o)]-(\mu_1+\mu_2)\cos(s_1\pi)} \tag{19}$$

Table 2 shows some sample results for β' where the modulus ratio used as examples correspond to Aluminum-Epoxy and Boron-Epoxy material pairs.

3. FINITE CRACKS

Referring now to Figure 7 we consider the bonded half planes containing two collinear cracks $(a_1<r<b_1, \theta=\theta_1)$ and $(a_2<r<b_2, \theta=\pi+\theta_1)$. It will be assumed that the crack surface tractions

$$\tau_{1\theta z}(r,\theta_1) = q_1(r), \tau_{2\theta z}(r,\theta_1+\pi) = q_2(r) \tag{20}$$

are the only external loads acting on the medium. The results for all other types of loading may be obtained through the standard superposition technique. Defining the unknown functions

$$f_i(r) = \frac{\partial}{\partial r}[w_i(r,\theta_i+0) - w_i(r,\theta_i-0)] \quad , \theta_2 = \pi + \theta_1 \quad , \quad i=1,2 \tag{21}$$

noting that (see Figure 7)

$$f_i(r) = 0 \quad , 0\leq r<a_i \quad , b_i<r<\infty \quad , i=1,2 \tag{22}$$

and using the standard dislocation solutions as the Green's functions [3], the problem may be reduced to the following system of integral equations:

$$q_1(\rho) = \frac{\mu_1}{2\pi}\int_{a_1}^{b_1} f_1(s)\{\frac{1}{s-\rho} - k(\rho,s,\theta_1)\}ds$$

$$- (1+\lambda)\frac{\mu_1}{2\pi}\int_{a_2}^{b_2} f_2(s)\frac{1}{\rho+s}ds \quad , (a_1<\rho<b_1) \quad ,$$

$$q_2(\rho) = \frac{\mu_2}{2\pi}\int_{a_2}^{b_2} f_2(s)\{\frac{1}{s-\rho} + k(s,\rho,\theta_1)\}ds$$

$$- (1-\lambda)\frac{\mu_2}{2\pi}\int_{a_1}^{b_1} f_1(s)\frac{1}{\rho+s}ds, \ (a_2<\rho<b_2) \tag{23a,b}$$

where

$$\lambda = (\mu_2-\mu_1)/(\mu_2+\mu_1) \quad , \tag{24}$$

$$k(\rho,s,\theta_1) = \frac{\lambda}{\rho+s} \frac{(\frac{\rho-s}{\rho+s})\sin^2\theta_1 + \cos^2\theta_1}{(\frac{\rho-s}{\rho+s})^2\sin^2\theta_1 + \cos^2\theta_1} \quad . \tag{25}$$

From (21) and (22) it follows that (23) must be solved under the following single-valuedness conditions:

$$\int_{a_i}^{b_i} f_i(r)dr = 0 \quad , \; i=1,2 \quad . \tag{26}$$

The solution of the system of singular integral equations is of the form

$$f_j(s) = \frac{G_j(s)}{(b_j-s)^{\alpha_j}(s-a_j)^{\beta_j}} \quad , \; j=1,2 \quad , \tag{27}$$

where $G_j(s)$ is a bounded function in the closed interval $a_j \leq s \leq b_j$. The coefficients α_j and β_j may be determined from the application of the function-theoretic method to the singular integral equations [4]. Thus it can be shown that

$$\alpha_1 = \alpha_2 = \frac{1}{2} \quad ,$$

$$\beta_1 = \beta_2 = \frac{1}{2} \quad , \text{ for } a_1>0 \quad , \; a_2>0 \quad ,$$

$$\beta_1 = \beta \quad , \; \beta_2 = \frac{1}{2} \quad , \text{ for } a_1 = 0 \quad , \; a_2>0 \quad ,$$

$$\beta_1 = \beta_2 = \beta' \quad , \text{ for } a_1 = 0 = a_2 \quad , \tag{28a-d}$$

where the real numbers β $(0<\beta<1)$ and β' $(0<\beta'<0.5)$ are the powers of stress singularity found in the previous section for a semi-

infinite crack and for a nonhomogeneous half plane, respectively*. (see tables 1 and 2).

The integral equations (23) are solved by introducing the following normalized quantities

$$t_j = \frac{2s - (b_j+a_j)}{b_j - a_j} \quad , \quad x_j = \frac{2\rho - (b_j+a_j)}{b_j - a_j} \quad ,$$

$$f_j(s) = \phi_j(t) = \frac{g_j(t)}{\left(\frac{b_j-a_j}{2}\right)^{\alpha_j+\beta_j} (1-t_j)^{\alpha_j} (1+t_j)^{\beta_j}} \quad .$$

$$q_j(\rho) = Q_j(x) \quad , \quad (-1 \leq (x_j, t_j) \leq 1) \quad , \quad (j = 1,2) \quad , \qquad (29)$$

and by using Gauss-Chebyshev or Gauss-Jacobi integration formulas (see, for example [5]). For crack geometries $a_1>0$ and $a_2 \geq 0$ or $a_1 \geq 0$, $a_2>0$ the conditions (26) are valid and the solution is rather straightforward. For $a_1 = 0 = a_2$ (26) reduces to the following condition

$$\int_0^{b_1} f_1(s)ds + \int_0^{b_2} f_2(s)ds = 0 \quad , \qquad (30)$$

stating that the crack surface displacements at r = 0 must be continuous. The additional condition which is necessary to insure the uniqueness of the solution of (23) comes from the function theoretic analysis (see, for example [5]) and is given by

$$\mu_1 G_1(0) = -G_2(0)\sqrt{b_1/b_2}\{(\mu_1-\mu_2)\cos[2(1-\beta_1)\theta_1] + (\mu_1+\mu_2)\cos[(1-\beta_1)\pi]\} \qquad (31)$$

*In this section it is assumed that $0<\theta_1<\frac{\pi}{2}$. Hence, if $\mu_1>\mu_2$, the characteristic function is $K_1(s) = 0$ as given by (13), and if $\mu_1<\mu_2$ then in (13) μ_1 and μ_2 are interchanged, where s_1 is the relevant root with $0<s_1<1$, $\beta' = 1-s_1$.

4. STRESS INTENSITY FACTORS

For the crack tips fully imbedded in a homogeneous medium, (i.e., for $a_1>0, a_2>0$) the stress intensity factors are defined by

$$k_3(b_i) = \lim_{r\to b_i}[2(r-b_i)]^{\frac{1}{2}}\tau_{i_{\theta z}}(r,\theta_i) \quad ,$$

$$k_3(a_i) = \lim_{r\to a_i}[2(a_i-r)]^{\frac{1}{2}}\tau_{i_{\theta z}}(r,\theta_i) \quad , \quad \theta_2 = \pi + \theta_1 \quad ,$$

$$i = 1,2 \, . \qquad (32)$$

For the crack terminating at an interface, for example, for $a_1 = 0, a_2>0$, k_3 is defined as

$$k_3 = \lim_{r\to 0}\sqrt{2}\, r^{\beta_1}\, \tau_{1_{\theta z}}(r,\theta_1) \, . \qquad (33)$$

For the crack crossing the interface, assuming that $0<\theta_1<\pi/2$, at the intersection of the crack and the interface stress state is singular only on one side of the crack. In this case the stress intensity factor is (arbitrarily) defined in terms of the interface shear stress as follows:

$$k_3^+(0) = \lim_{r\to 0}\sqrt{2}\, r^{\beta_1}\, \tau_{1_{\theta z}}(r,\pi/2) \quad , \quad k_3^-(0) = 0 \quad , \text{ for } \mu_1>\mu_2 \quad ,$$

$$k_3^-(0) = \lim_{r\to 0}\sqrt{2}\, r^{\beta_1}\, \tau_{1_{\theta z}}(r,-\pi/2) \quad , \quad k_3^+(0) = 0 \quad , \text{ for } \mu_1<\mu_2 \, .$$

(34a,b)

In the numerical analysis the stress intensity factors are obtained in terms of asymptotic values of the functions $f_i(r)$ and $f_2(r)$ or in terms of $g_j(\mp 1)$, $(j = 1,2)$ (see equation (29)).

The calculated results given in the next section is based on constant crack surface tractions, namely

$$q_i(r)=Q_i(x)= q_{io} \quad , \ a_i<r<b_i \quad , \ -1<x<1 \quad , \ i = 1,2. \tag{35}$$

For example, if the nonhomogeneous plane is under uniform anti-plane shear

$$\tau_{1xz}(\infty,y) = \tau_{2xz}(-\infty,y) = q_o \tag{36}$$

then

$$q_{10} = -q_o\sin\theta_1 \quad , \ q_{20} = q_o\sin\theta_1 \quad . \tag{37}$$

Or, if the plane is under displacement loading

$$\frac{\partial w_1}{\partial y} = \frac{\partial w_2}{\partial y} = \varepsilon_o \quad , \ y\to\mp\infty \quad , \tag{38}$$

then

$$q_{10} = -\mu_1\varepsilon_o\cos\theta_1 \quad , \ q_{20} = \mu_2\varepsilon_o\cos\theta_1 \quad . \tag{39}$$

5. NUMERICAL RESULTS

The numerical results for a crack lying in one half plane only (i.e., for $a_2 = b_2$) are given in Tables 3-5 where

$$a_0 = (a_1+b_1)/2 \quad , \ c = a_1 + a_0. \tag{40}$$

The tables show the normalized stress intensity factors defined by

$$K(+1) = \frac{k_3(b_1)}{q_{10}\sqrt{a_o}} \quad , \tag{41}$$

$$K(-1) = \begin{cases} \dfrac{k_3(a_1)}{q_{10}\sqrt{a_0}} & , \text{ for } c>a_0 \quad , \\ \dfrac{k_3(0)}{a_0^{\beta_1}q_{10}} & , \text{ for } c = a_0 \quad . \end{cases} \tag{42}$$

The material pair of aluminum and epoxy is used as an example. In Table 3 $\mu_2>\mu_1$, in Table 4 $\mu_2<\mu_1$, and in Table 5 $\mu_2 = 0$ (the half plane). For the crack tip terminating at the interface

(i.e., for $a_1 = 0$ or $c = a_0$) the corresponding power $\beta_1 = \beta$ of the stress singularity is given in Table 1.

The results for the problem of a crack crossing the boundary are given in Table 6. In this case the normalized stress intensity factors shown in the table are defined by

$$K_3(b_1) = \frac{k_3(b_1)}{q_{10}\sqrt{b_1}} \quad , \quad K_3(b_2) = \frac{k_3(b_2)}{q_{20}\sqrt{b_1}}$$

$$K_3^-(0) = \frac{k_3^-(0)}{q_{20} b_1^{\beta_1}} \quad . \qquad (43a\text{-}c)$$

In this example the external loads are assumed to be the displacement loading given by (38) and (39). Note that since $\mu_1 < \mu_2$ and $0 < \theta_1 < \pi/2$, $k_3^+(0) = 0$. The related power of stress singularity $\beta_1 = \beta'$ is given by Table 2.

Figures 8 and 9 show some sample distributions of the density functions f_1 and f_2 for $a_1 = a_2 = 0$ which are normalized in the following form:

$$F_i(t_i) = 2\varepsilon_0 \left(\frac{b_1}{2}\right)^{\beta_1 + \frac{1}{2}} f_i(r) \quad ,$$

$$-1 < t_i < 1 \quad , \quad 0 < r < b_i \quad , \quad i = 1,2 \qquad (44)$$

where ε_0 is the load parameter defined by (38). Note that at $r = 0$ or $t_i = -1$ the density functions become unbounded having a common $r^{-\beta_1}$ type singularity.

Figures 10 and 11 give some idea about the crack opening displacement again for the case of a crack crossing the interface. Here, the normalized displacements W_1 and W_2 are defined by

$$W_i(t_i) = 2(-1)^i \varepsilon_0 \left(\frac{b_1}{2}\right)^{\beta_1 + \frac{1}{2}} [w_i^+ - w_i^-] \quad , \quad i = 1,2 \quad . \qquad (45)$$

Table 3. Normalized stress intensities for $\mu_2/\mu_1 = 23.08$ for crack approaching and terminating at a bimaterial interface.

c/a_o	$\theta_1 = 0$		$\theta_1 = \frac{\pi}{8}$		$\theta_1 = \frac{\pi}{4}$		$\theta_1 = \frac{3\pi}{8}$	
	K(+1)	K(-1)	K(+1)	K(-1)	K(+1)	K(-1)	K(+1)	K(-1)
1.00	0.907	14.0	0.902	4.56	0.885	2.06	0.847	1.36
1.05	0.916	0.610	0.911	0.611	0.893	0.622	0.852	0.659
1.10	0.924	0.712	0.919	0.706	0.900	0.693	0.857	0.696
1.15	0.931	0.770	0.925	0.761	0.906	0.737	0.862	0.719
1.25	0.941	0.837	0.936	0.826	0.916	0.794	0.869	0.752
1.50	0.959	0.911	0.954	0.901	0.936	0.869	0.886	0.804
2.00	0.976	0.959	0.973	0.953	0.959	0.931	0.913	0.865
5.00	0.996	0.995	0.995	0.994	0.992	0.990	0.975	0.970
10.00	0.999	0.999	0.999	0.999	0.998	0.998	0.993	0.992
∞	1.0	1.0	1.0	1.0	1.0	1.0	1.0	1.0

Table 4. Normalized stress intensities for $\mu_2/\mu_1 = 0.0433$ for crack approaching and terminating at a bimaterial interface.

c/a_o	$\theta_1 = 0$		$\theta_1 = \frac{\pi}{8}$		$\theta_1 = \frac{\pi}{4}$		$\theta_1 = \frac{3\pi}{8}$	
	K(+1)	K(-1)	K(+1)	K(-1)	K(+1)	K(-1)	K(+1)	K(-1)
1.00	1.26	0.0767	1.28	0.0824	1.33	0.105	1.49	0.172
1.05	1.13	1.70	1.15	1.74	1.19	1.87	1.34	2.22
1.10	1.11	1.44	1.12	1.47	1.16	1.58	1.30	1.87
1.15	1.09	1.32	1.10	1.35	1.14	1.44	1.28	1.71
1.25	1.07	1.21	1.08	1.23	1.12	1.30	1.24	1.53
1.50	1.05	1.10	1.05	1.12	1.08	1.17	1.18	1.33
2.00	1.03	1.04	1.03	1.05	1.05	1.08	1.12	1.18
5.00	1.00	1.00	1.01	1.01	1.01	1.01	1.03	1.03
10.00	1.00	1.00	1.00	1.00	1.00	1.00	1.01	1.01
∞	1.00	1.00	1.00	1.00	1.00	1.00	1.00	1.00

Table 5. Normalized stress intensity factors for crack approaching a free boundary, $\mu_2 = 0$.

c/a_o	$\theta_1 = 0$		$\theta_1 = \frac{\pi}{8}$		$\theta_1 = \frac{\pi}{4}$		$\theta_1 = \frac{3\pi}{8}$	
	K(+1)	K(-1)	K(+1)	K(-1)	K(+1)	K(-1)	K(+1)	K(-1)
1.05	1.15	1.79	1.17	1.84	1.22	2.01	1.40	2.48
1.10	1.12	1.49	1.13	1.53	1.18	1.66	1.35	2.03
1.15	1.10	1.36	1.12	1.39	1.16	1.50	1.32	1.82
1.20	1.09	1.28	1.10	1.31	1.14	1.40	1.29	1.70
1.25	1.08	1.23	1.09	1.25	1.13	1.34	1.27	1.60
1.50	1.05	1.11	1.06	1.13	1.09	1.18	1.20	1.37
2.00	1.03	1.05	1.03	1.06	1.05	1.09	1.13	1.20
5.00	1.00	1.01	1.01	1.01	1.01	1.01	1.03	1.04
10.00	1.00	1.00	1.00	1.00	1.00	1.00	1.01	1.01
∞	1.00	1.00	1.00	1.00	1.00	1.00	1.00	1.00

Table 6. Normalized stress intensities for crack through the interface, $\mu_2/\mu_1 = 23.08$.

$b_2/b_1 \rightarrow$		0.05	0.5	1.0	2.0	20.0
$\theta_1 = 0$	$K_3(b_1)$	0.645	0.780	1.00	1.52	11.1
	$K_3(b_2)$	0.249	0.721	1.00	1.40	4.27
	$K_3^-(0)$	0	0	0	0	0
$\theta_1 = \frac{\pi}{8}$	$K_3(b_1)$	0.642	0.781	1.01	1.54	11.4
	$K_3(b_2)$	0.253	0.730	1.02	1.42	4.32
	$K_3^-(0)$	-0.0574	-0.00497	0.0255	0.0647	0.604
$\theta_1 = \frac{\pi}{4}$	$K_3(b_1)$	0.631	0.790	1.05	1.65	12.7
	$K_3(b_2)$	0.266	0.765	1.06	1.48	4.49
	$K_3^-(0)$	-0.0289	0.0242	0.0533	0.0987	0.727
$\theta_1 = \frac{3\pi}{8}$	$K_3(b_1)$	0.607	0.831	1.19	1.99	16.3
	$K_3(b_2)$	0.306	0.871	1.21	1.68	5.01
	$K_3^-(0)$	-0.00653	0.0692	0.113	0.181	1.07

It should be emphasized that at the interface even though the displacements W_1 and W_2 are continuous, their derivatives are always discontinuous. This means that at r = 0 the crack opening displacement would always have a "kink".

REFERENCES

1. F. Erdogan and T.S. Cook, "Antiplane Shear Crack Terminating at and going through a bimaterial interface," Int. J. of Fracture, Vol. 10, pp 227-240 (1974)

2. F. Erdogan and G.D. Gupta, "Bonded Wedges with an Interface Crack Under Antiplane Shear Loading," Int. J. of Fracture, Vol. 11, pp 583-593 (1975)

3. J. Dundurs, "Elastic Interaction of Dislocations with Inhomogeneities," Mathematical Theory of Dislocations, T. Mura, ed., pp 70-115 (1969)

4. N.I. Muskhelishvili, Singular Integral Equations, P. Noordhoff, Guoningen, The Netherlands (1953)

5. F. Erdogan, "Mixed Boundary Value Problems in Mechanics," Mechanics Today, Vol. 4, S. Nemat-Nasser, ed., Pergamon Press, Oxford (1978)

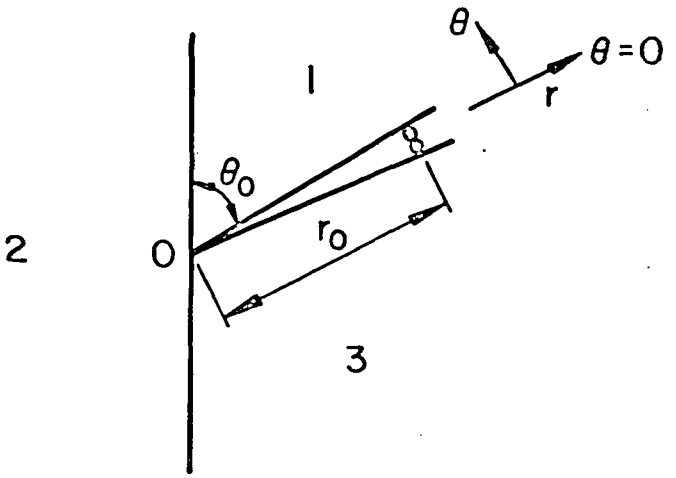

Figure 1. Semi-infinite crack terminating at a bimaterial interface in bonded half planes.

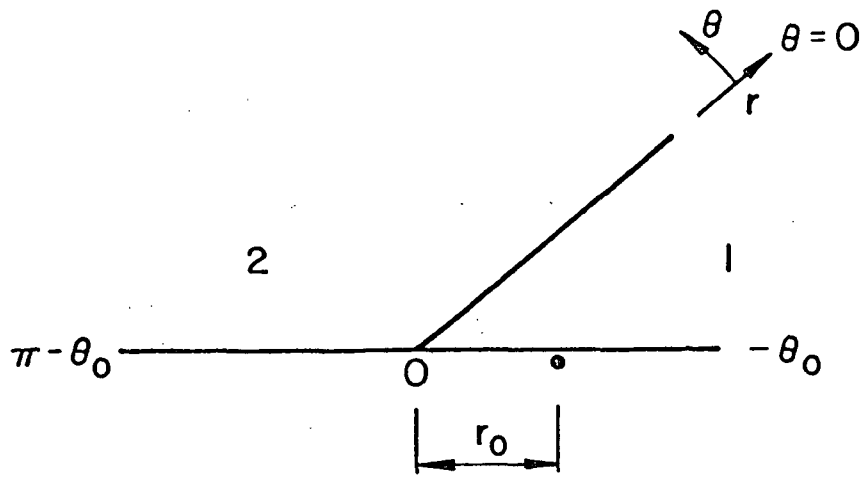

Figure 2. Half plane which consists of two dissimilar bonded wedges.

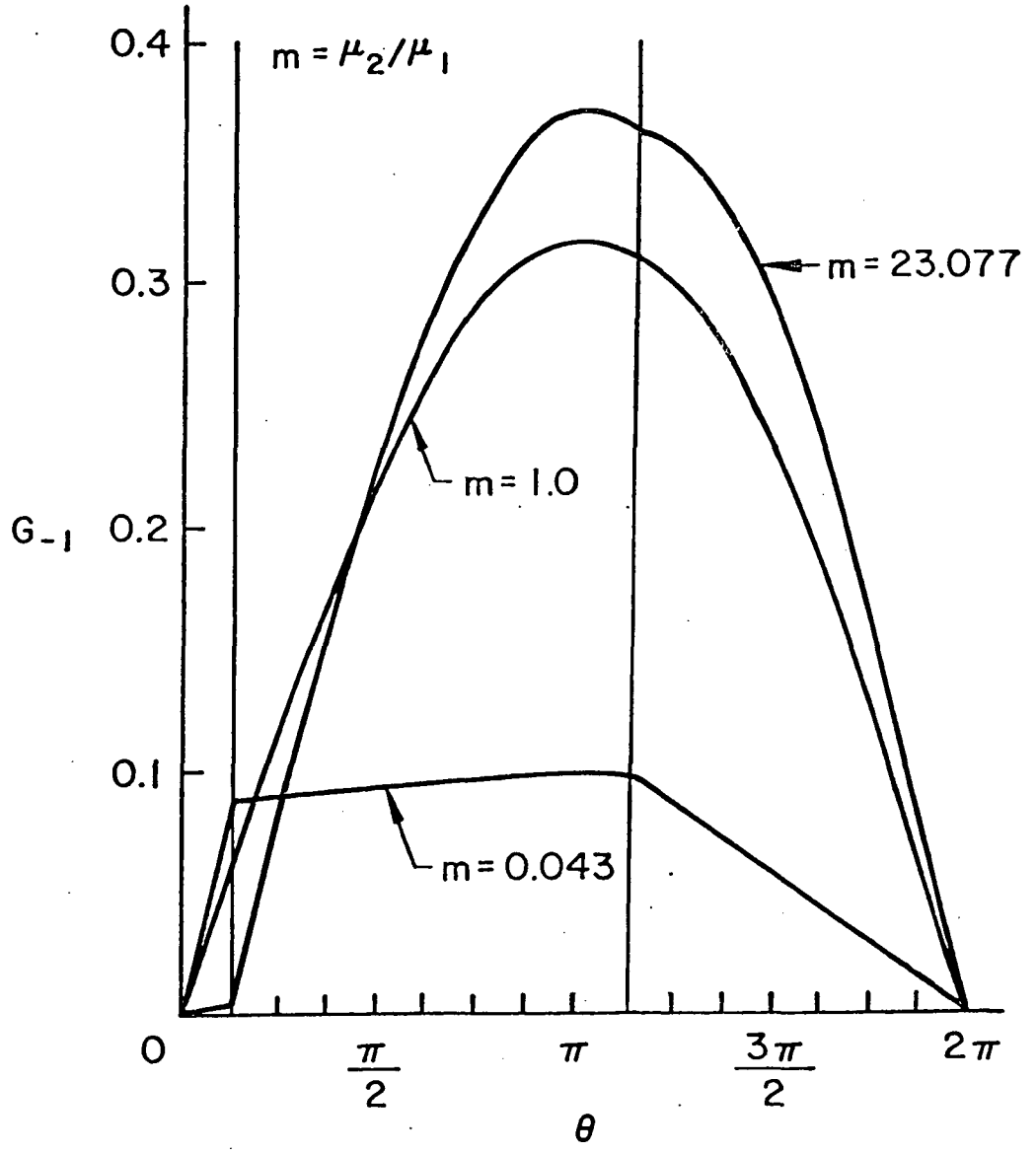

Figure 3. Angular distribution of the measure of shear cleavage stress $\tau_{\theta z}$ in bonded half planes with a semi-infinite crack (see Figure 1 and equation 5 for terminology). Material pair: Aluminum-Epoxy, $\theta_o = \pi/8$.

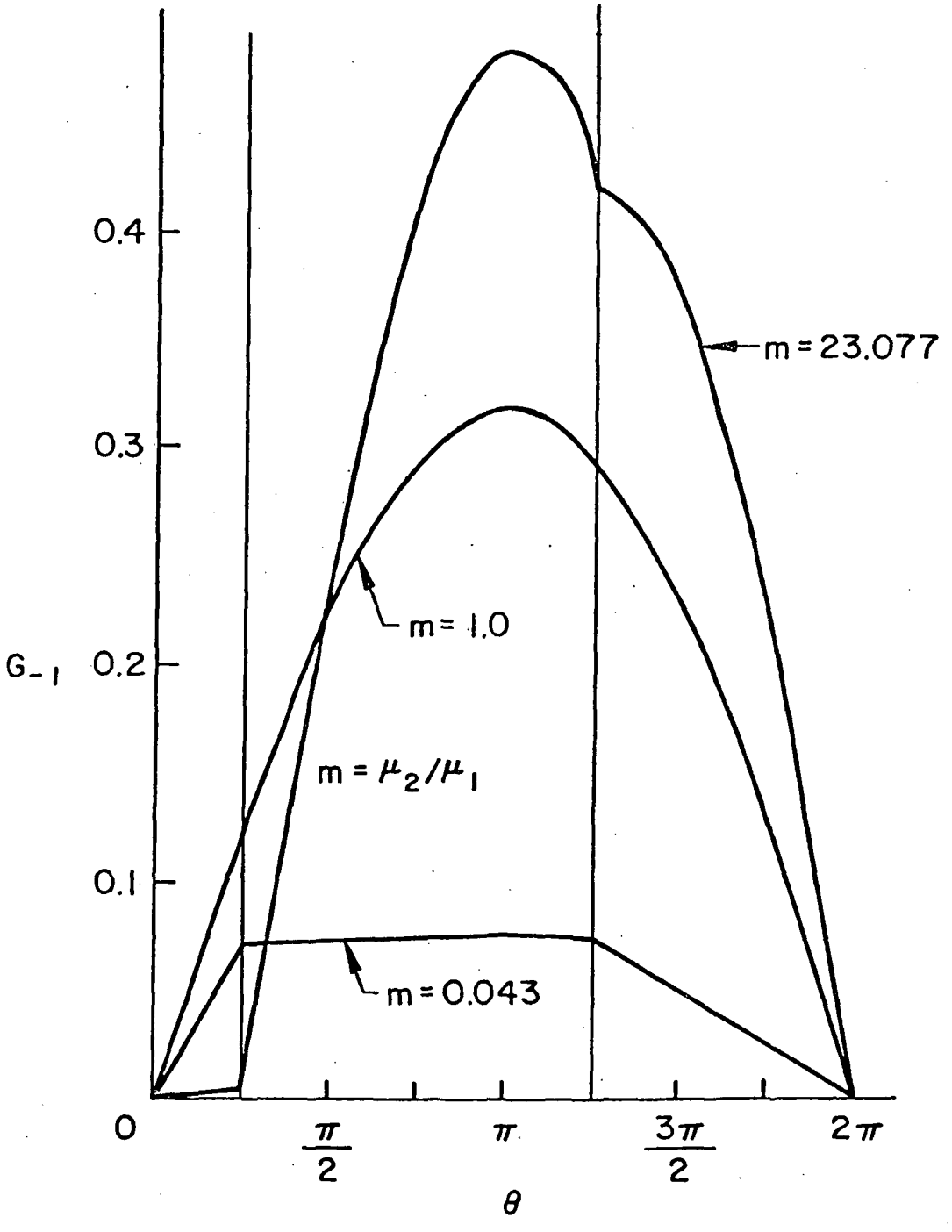

Figure 4. Same as Figure 3, $\theta_0 = \pi/4$

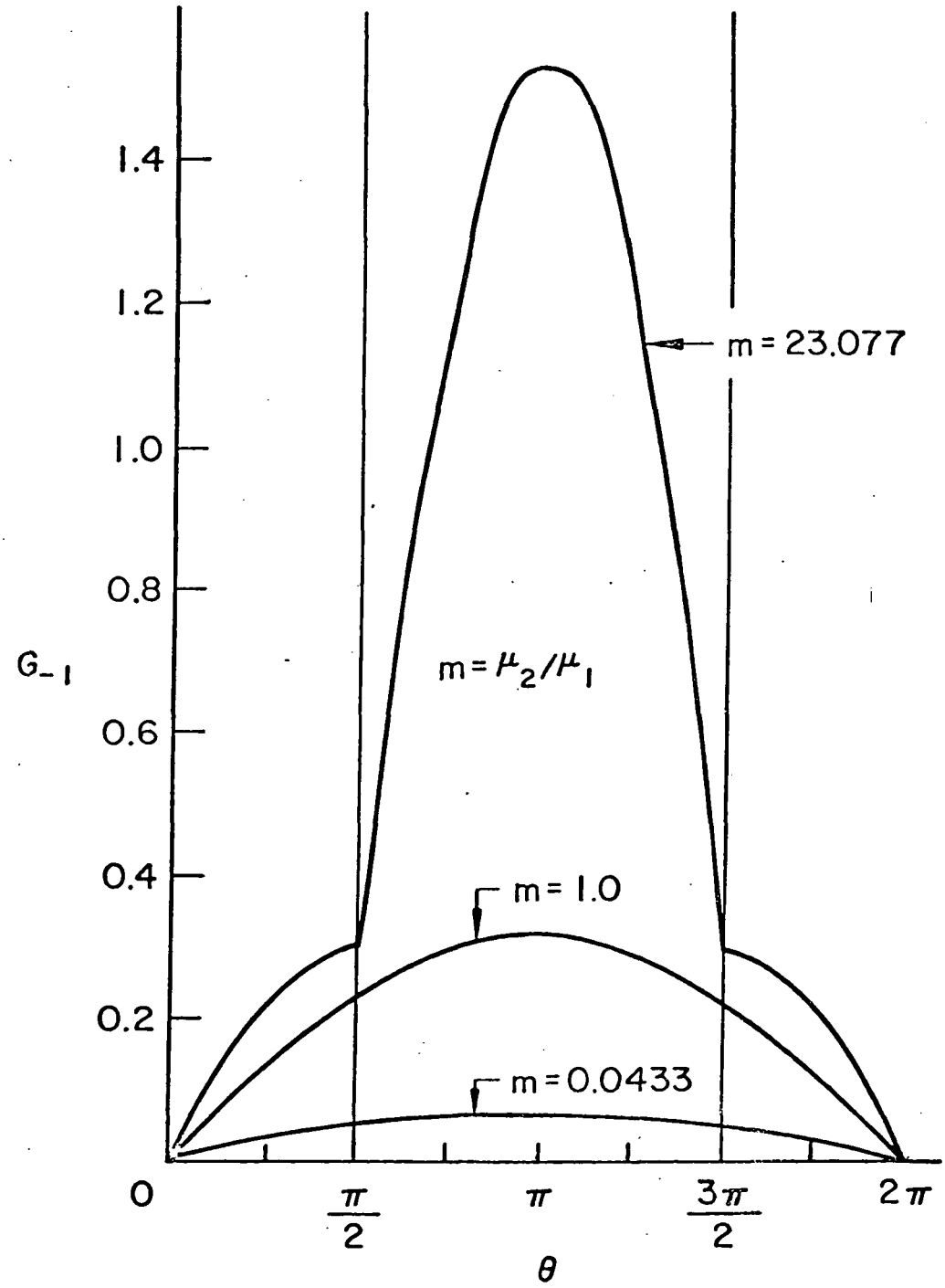

Figure 5. Same as Figure 3, $\theta_0 = \pi/2$.

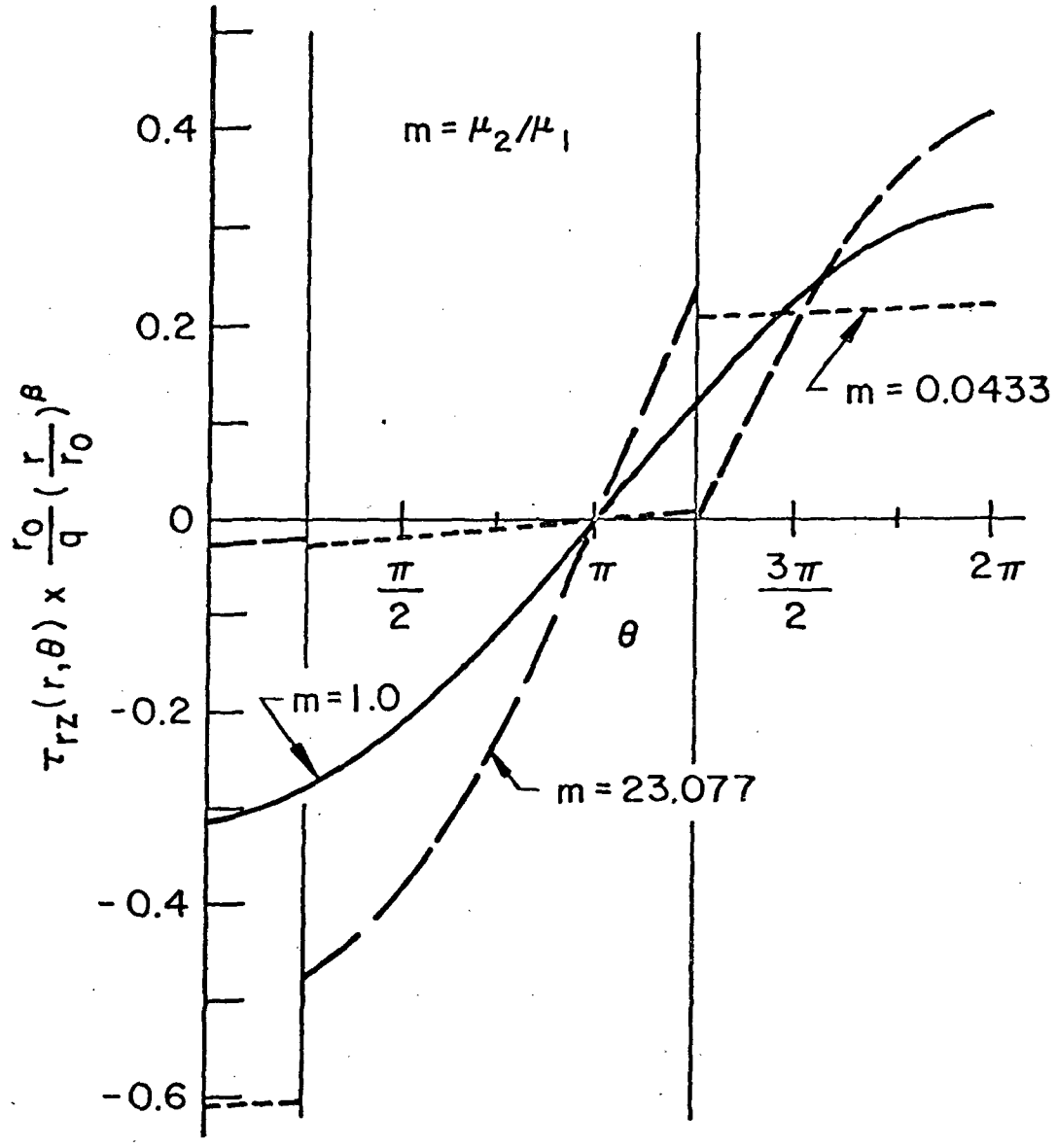

Figure 6. Angular distribution of the stress component τ_{rz} for $\theta_0 = \pi/4$ (see Figure 1 for terminology).

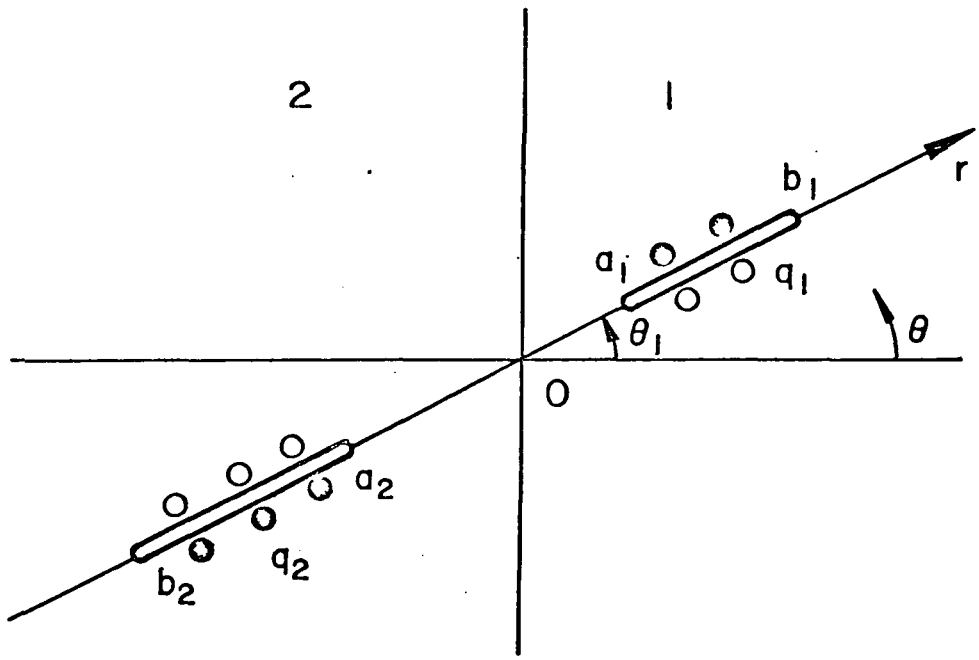

Fig. 7 Bonded half planes containing arbitarily located collinear cracks.

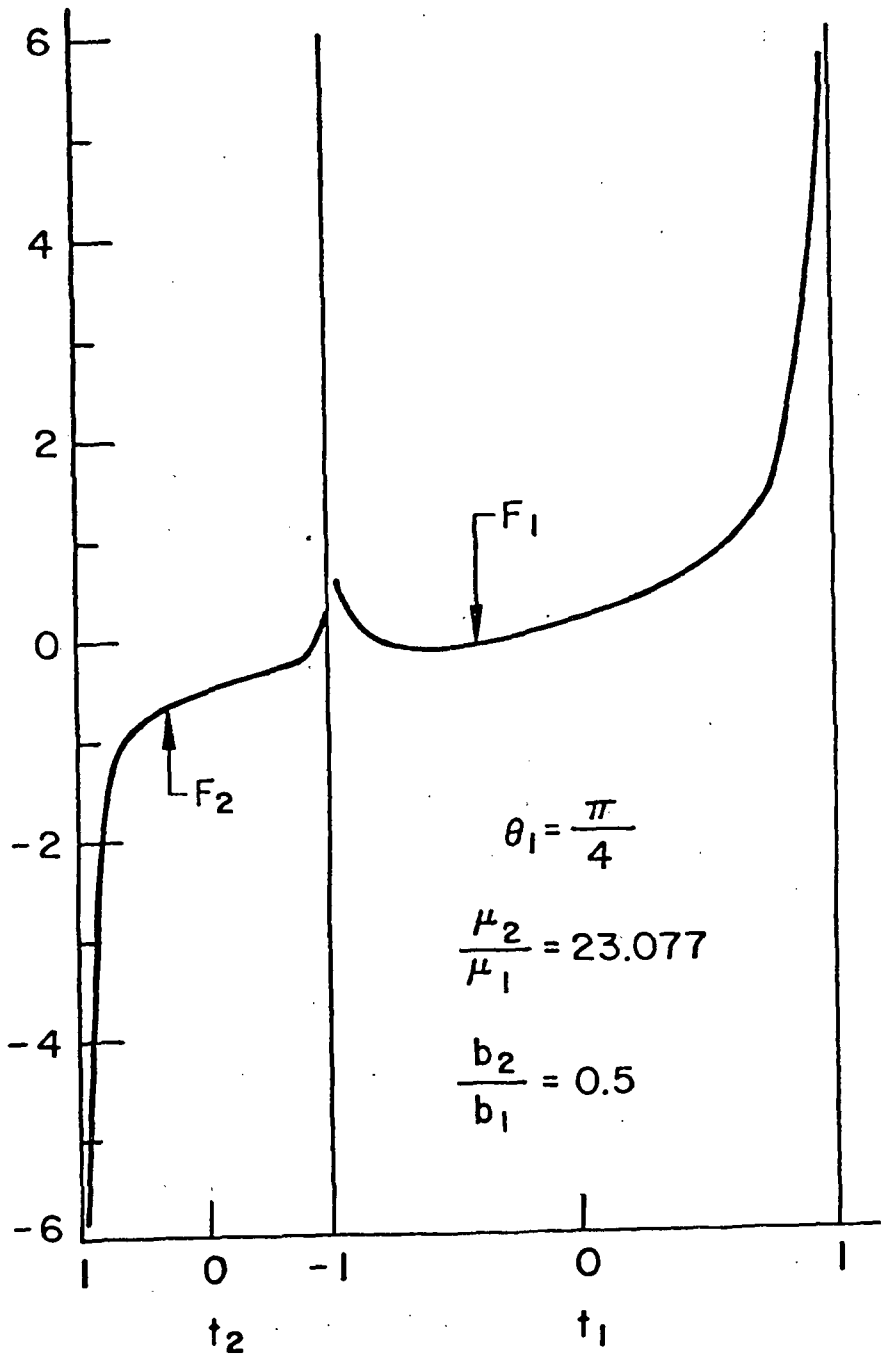

Figure 8. Distribution of the normalized density functions in bonded half planes with a crack crossing the interface (see equations 21, 29 and 44 and Figure 7 for definitions).

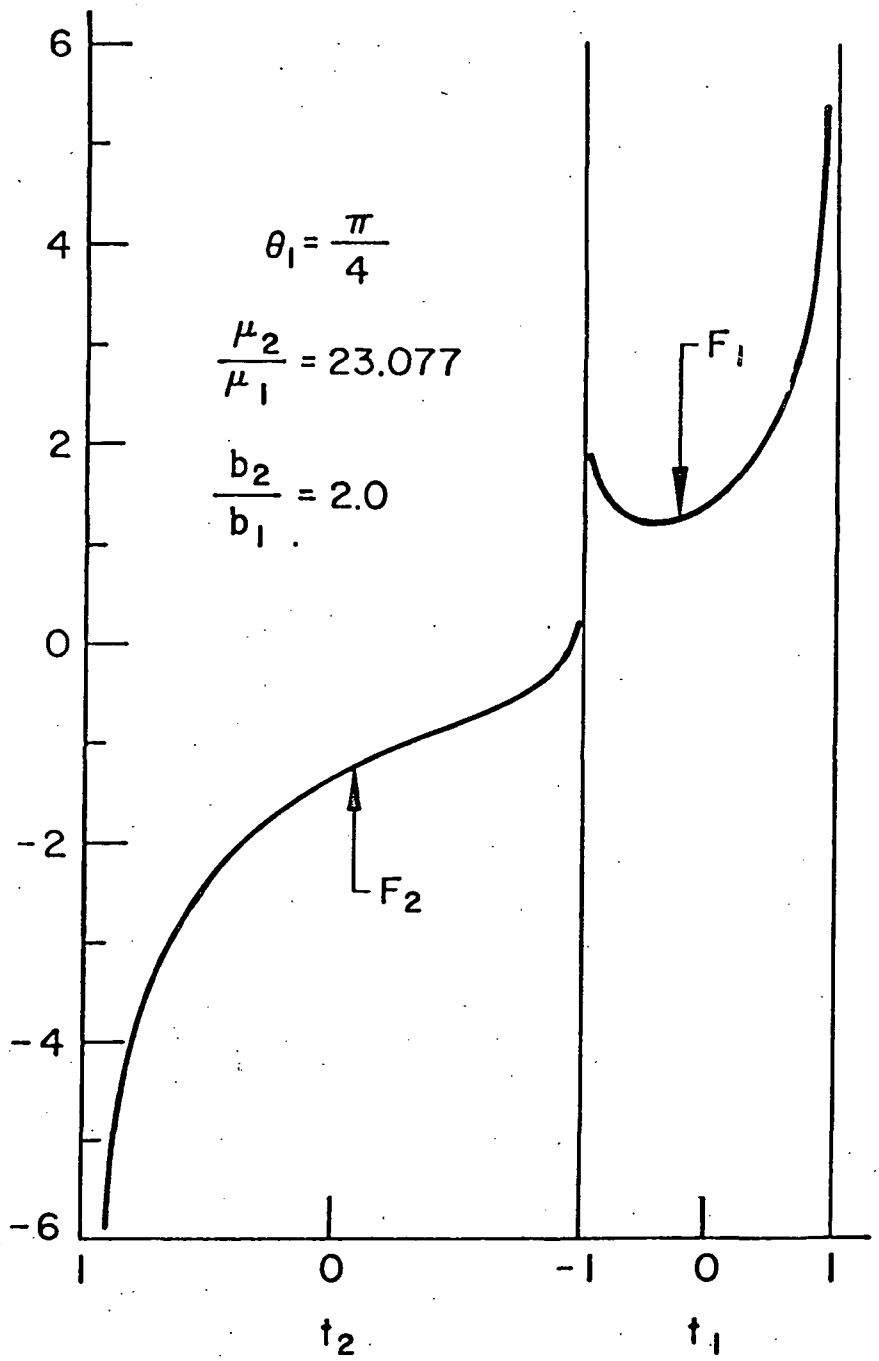

Figure 9. Same as Figure 8, $b_2/b_1 = 2$.

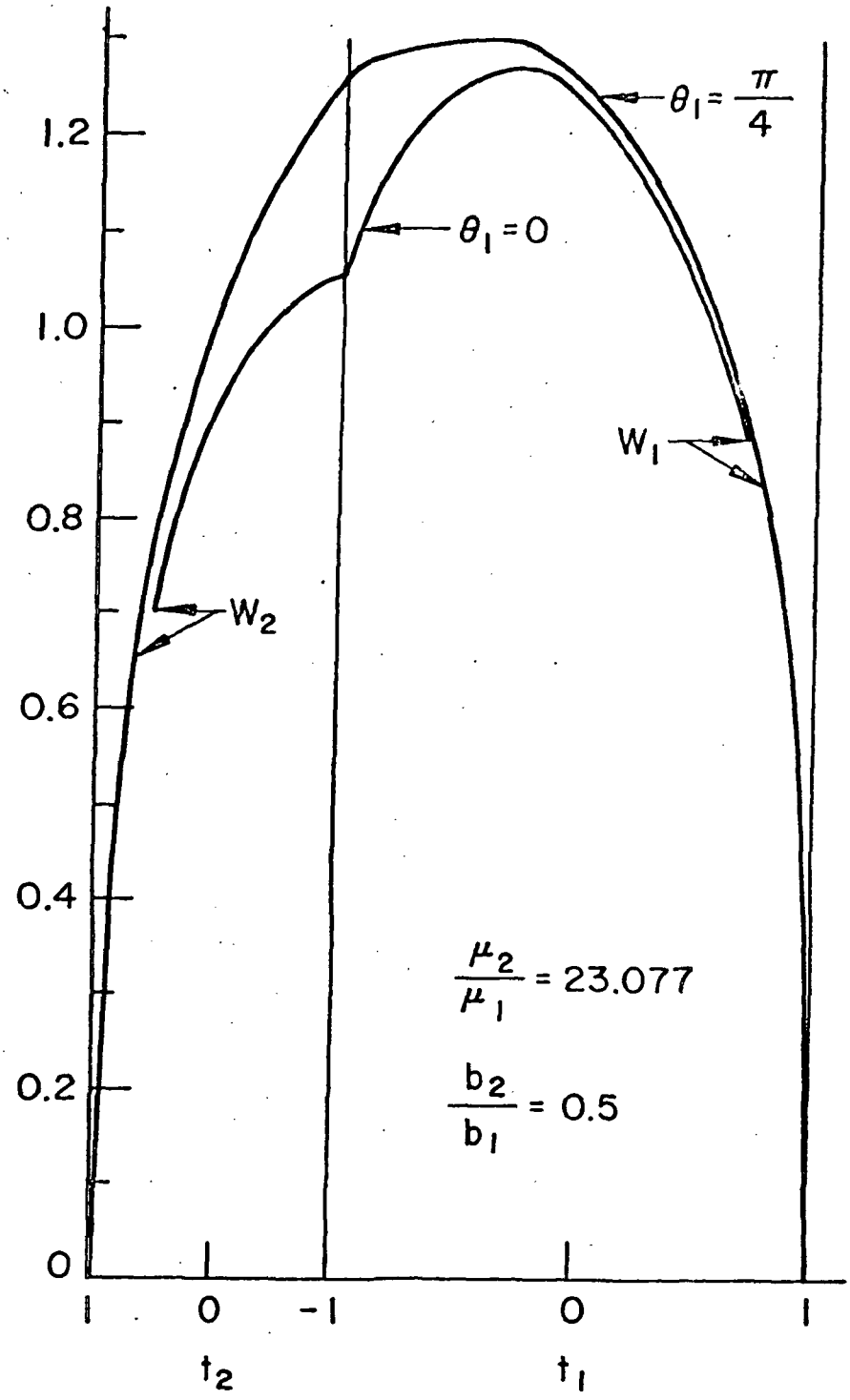

Figure 10. Distribution of the normalized crack opening displacement in bonded half planes with a crack crossing the interface (see equations 45 and 29, and Figure 1 for definitions).

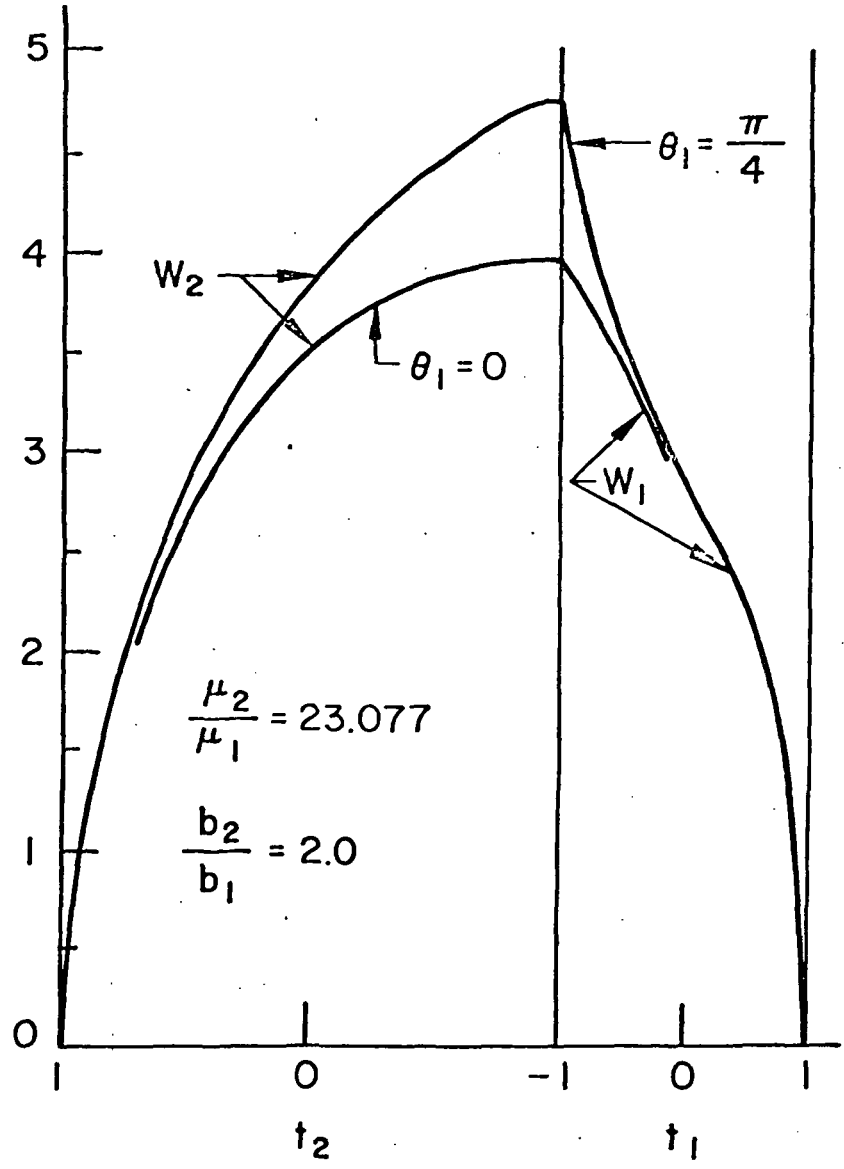

Figure 11. Same as Figure 10, $b_2/b_1 = 2$.